ELSEVIER

Journal of Power Sources 113 (2003) 308–317

JOURNAL OF POWER SOURCES

www.elsevier.com/locate/jpowsour

Electrochemical behavior of lead alloys in sulfuric and phosphoric acid solutions

I. Paleska[a], R. Pruszkowska-Drachal[a], J. Kotowski[a], A. Dziudzi[a], J.D. Milewski[c], M. Kopczyk[c], A. Czerwiński[a,b,c,*]

[a]*Department of Chemistry, Warsaw University, Pasteura 1, 02-093 Warsaw, Poland*
[b]*Industrial Chemistry Research Institute, Rydygiera 8, 01-793 Warsaw, Poland*
[c]*Central Laboratory of Cells and Batteries, 61-362 Poznan, Poland*

Abstract

The electrochemical behavior of lead, lead–antimony, and lead–calcium–aluminium–tin alloys has been studied in solutions containing various concentrations of sulfuric and phosphoric acids. The dependence of these electrode processes on some experimental conditions (mainly sweep rate and potential range) has been studied. The measurements were performed using a cyclic voltammetry technique. The study and the analysis of the morphology of alloys have been performed using a scanning electron microscope (SEM). Cyclic voltammograms of the lead–antimony alloy electrodes, similarly to pure lead electrode, also show the ''anodic excursion'' peak under some experimental conditions. Well defined current waves, corresponding to the oxidation and reduction processes of Sb, are observed, if the alloy surface is freshly abraded. The oxidation of antimony starts at potentials at which the formation of PbO takes place. The peak current of Sb oxidation reaction decreases during successive cycles, suggesting that Sb dissolves from the alloy surface during the first CV sweeps. Another explanation for this effect might be the formation of a $PbSO_4$ selective membrane.

Keywords: Lead; Lead dioxide; Electrochemistry of lead alloys

1. Introduction

One of the curiosities of the redox reactions of the lead electrode is the appearance of small oxidation peaks that accompany the main reduction process, attributed to the reduction of lead dioxide to lead sulfate [1–14]. These small anodic peaks, sometimes [3,4] called ''anodic excursion'' peaks, appear either before [2,8] or after [3,4] the main reduction peak, and depend significantly on the conditions of the experiment. The presence of the ''anodic excursion'' peaks has been explained in the literature in many different ways [1–15]. The effect of the ''excursion peak'' appearance has been examined in details in sulfuric acid solutions with various concentrations (0.05–5 M) in a wide range of sweep rates, potential polarization and temperature [15]. Since all these peaks appear on the CVs only when the electrode potential is cycled in a wide potential range, limited by hydrogen and oxygen evolution, it has been proposed that they are related to the reduction of lead dioxide to the bare metal, occurring at high negative potentials. The presence of a small reduction peak preceding ''anodic excursion'' peaks, as well as the presence of the main reduction peak of the lead dioxide has also been related to the exposure of the bare metal.

As suggested by Deutscher et al. [4], when the lead dioxide, formed at high positive potentials, is reduced ($PbO_2 \rightarrow PbSO_4$), a large increase of the molar volume is expected and, as a result, the surface cracks, exposing the bare metal. These parts of the surface are then oxidized in ''anodic excursion'' peaks. To repeat these redox processes, the electrode has to be reduced again at high negative potentials, i.e. at the conditions when reduction to the metal occurs. The CVs performed only in a positive potential range confirmed that the reduction of PbO_2 to $PbSO_4$, which follows the formation of PbO_2, is not related to the ''anodic excursion'' peaks and it also means that no cracks of the surface occur, as long as the potential cycling of the electrode to high negative potentials, and the resulting reduction to the metal, are avoided. Therefore, when the lead electrode is used as a positive electrode in a battery, no corrosion due to the exposure of the bare metal is expected.

The knowledge of the electrochemical behavior of lead–antimony an lead–other metals alloys is important from the

* Corresponding author. Fax: +48-22-8225996.
E-mail address: aczerw@chem.uw.edu.pl (A. Czerwiński).

0378-7753/02/$ – see front matter
PII: S0378-7753(02)00530-X

point of view of these alloys application as a material for grid construction in lead-acid batteries. This problem has been studied by many authors [16–32].

The influence of phosphoric acid on lead/sulfuric acid system has been studied for more than 70 years [32–36], but this problem is still not fully understood. It is known that the addition of phosphoric acid to sulfuric acid changes the features of cyclic voltammograms of lead [32,33] and improves the performance of lead/acid battery [34].

In this report, the influence of phosphoric acid, and its additions to sulfuric acid, on the electrochemical behavior (especially the presence of the ''anodic excursion'' peak) of lead, lead–antimony and lead–calcium–aluminum–tin alloys is presented. The sulfuric acid (5.0 M) with 2 and 10% phosphoric acid additions and pure phosphoric acid (0.5 and 5.0 M) solutions were used in this work.

2. Experimental

The working electrode was a wire from lead, lead–antimony 1.7 and 3% Sb) and lead–calcium–aluminum–tin alloys (0.085% Ca, 0.002% Al, 0.765% Sn; 0.5 cm^2 of geometric area). The sulfuric acid solutions with various molar concentrations (0.5 and 5.0 M) were used as the electrolytes. The phosphoric acid solutions with 0.5 and 5.0 M concentrations were also used as the electrolytes. The sulfuric acid (5.0 M) with 2 and 10% phosphoric acid addition and phosphoric acid (0.5 and 5.0 M) solutions were used. These solutions were de-aerated with argon and the experiments were carried out in a glass cell. The cyclic voltammograms were obtained at sweep rates ranging from 10 to 100 mV/s. The experiments were carried out at room temperature (298 K).

Cyclic voltammograms of a pure Pb-wire electrode in aqueous phosphoric acid solutions (0.5–5.0 M) in the potential region between hydrogen and oxygen evolution were obtained at a constant sweep rate (50 mV/s). Before the experiment, the electrode was mechanically polished with abrasive paper (P500 and P1000), washed in acetone and thoroughly rinsed in triply distilled water. Before the start of the cyclic voltammetric experiments, i.e. prior to each run, the lead electrode was reduced at the potential of hydrogen evolution for about 5 min. In some experiments the electrode was polarized at the potentials at which PbO_2 generation was completed (i.e. ca. 2.4 V). Usually, the potential of the lead alloy electrode was cycled between −2.0 and 2.4 V. In some experiments, the potential range of the electrode polarization was limited. The counter electrode was a platinum black foil (ca. 4 cm^2 geometric area) and the reference electrode was a Hg, Hg_2SO_4, $K_2SO_{4(sat)}$ (0.680 V vs. NHE).

Micrographs of lead and lead alloy electrodes were obtained with a scanning electron microscope (SEM) LEO 435 VP.

3. Results and discussion

The redox reactions occurring on the Pb alloy electrodes in sulfuric and phosphoric acid solutions are complex and depend on many variables, such as the concentration of the acids, or the sweep rate in cyclic voltammetry experiments. In this paper, particular attention will be paid to the potential range where processes responsible for ''anodic excursion'' peak formation take part.

3.1. The electrochemical behavior of lead in sulfuric and phosphoric acid solutions

Fig. 1 shows initial cyclic voltammetric scans (1, 5 and 10), at 50 mV/s, of a pure lead wire electrode cycled in 0.5 M H_2SO_4 in the potential range limited by the evolution of hydrogen and oxygen.

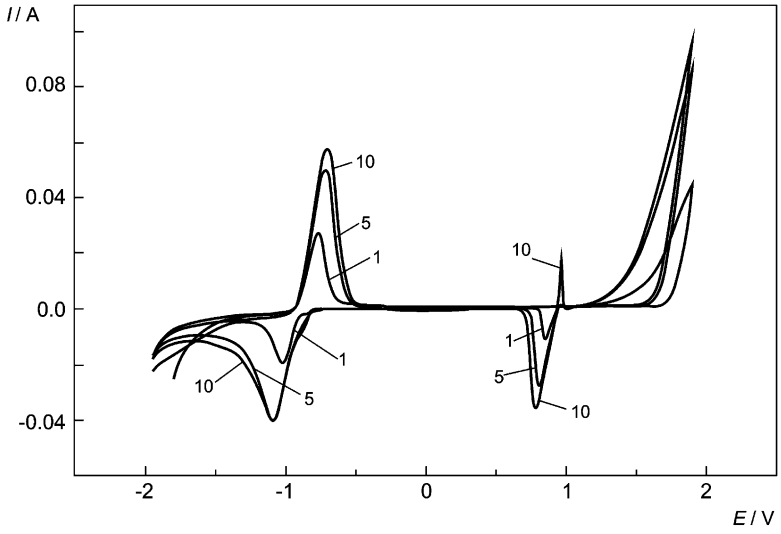

Fig. 1. Cyclic voltammograms at 50 mV/s of Pb electrode in 0.5 M H_2SO_4. 1, 5, 10-numbers of the cycle.

In Fig. 2a and b the scanning electron micrographs (SEM) of the lead electrode after the first (Fig. 2a) and the tenth cycle (Fig. 2b) of polarization in sulphuric acid are demonstrated.

The increase of the current, shown in Fig. 1, suggests that the real surface increases during the cyclic polarization of the electrode. The SEM images (Fig. 2a and b) confirm this conclusion. The morphology of the lead electrode surface at

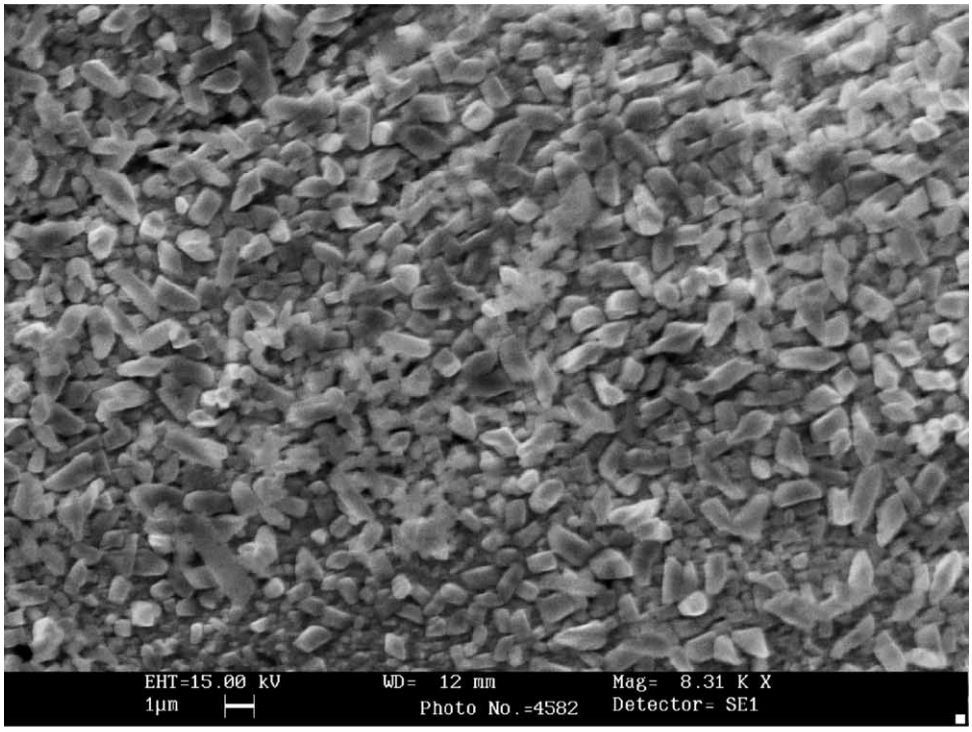

(a)

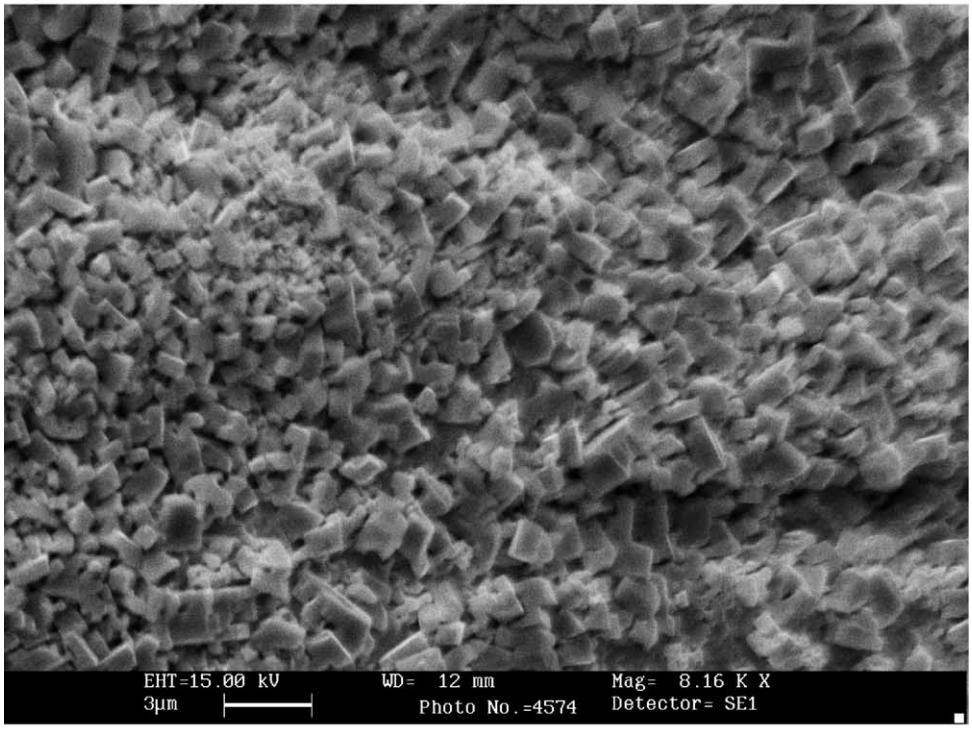

(b)

Fig. 2. (a) The SEM of lead electrode after the first cycle of polarization in 0.5 M H_2SO_4. Starting potential: −1.95 V. (b) The SEM of lead electrode after the tenth cycle of polarization in 0.5 M H_2SO_4. Starting potential: −1.95 V.

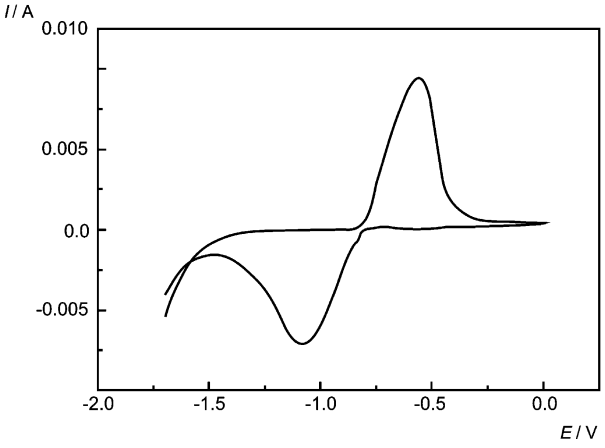

Fig. 3. Cyclic voltammogram at 50 mV/s of Pb electrode in 0.5 M H_3PO_4.

the beginning and at the end of cyclic polarization is changed. The surface becomes more rough and the sizes of the crystals formed are getting smaller. These effects are reflected by current density increases during cyclic electrode polarization.

Fig. 3 shows the cyclic voltammogram of pure lead cycled in phosphoric acid in a potential range from −1.7 to 0.0 V, i.e. where the oxidation of lead to hydrophosphates and their reduction to metal occurs (Pb ⇔ $PbHPO_4$) [35]. The ratio of charges needed for lead oxidation, [Pb ⇒ Pb(II), Q_a] and lead(II) reduction [Pb(II) ⇒ Pb, Q_c], is higher than unity ($Q_a/Q_c > 1$). This result suggests that this oxidation–reduction process is not fully reversible and some amount of lead(II) is not reduced completely during the cathodic scan.

Fig. 4a and b shows the dependence of the anodic charges of a pure lead wire electrode Q_a, obtained at various sweep rates, on the number of potential scans from −1.7 to 0.0 V in 0.5 M H_3PO_4 (Fig. 4a) and in 1.0 M H_3PO_4 (Fig. 4b) solutions. It can clearly be seen from these figures that the process of lead oxidation is enhanced for higher acid concentration (1.0 M) and lower rate of electrode polarization (10 mV/s).

The scanning electron images of the lead electrode after oxidation and reduction followed by an oxidation process are demonstrated in Figs 5a and b, respectively. It can clearly be seen that some amount of $PbHPO_4$ crystals formed during oxidation process is not reduced during lead electrode

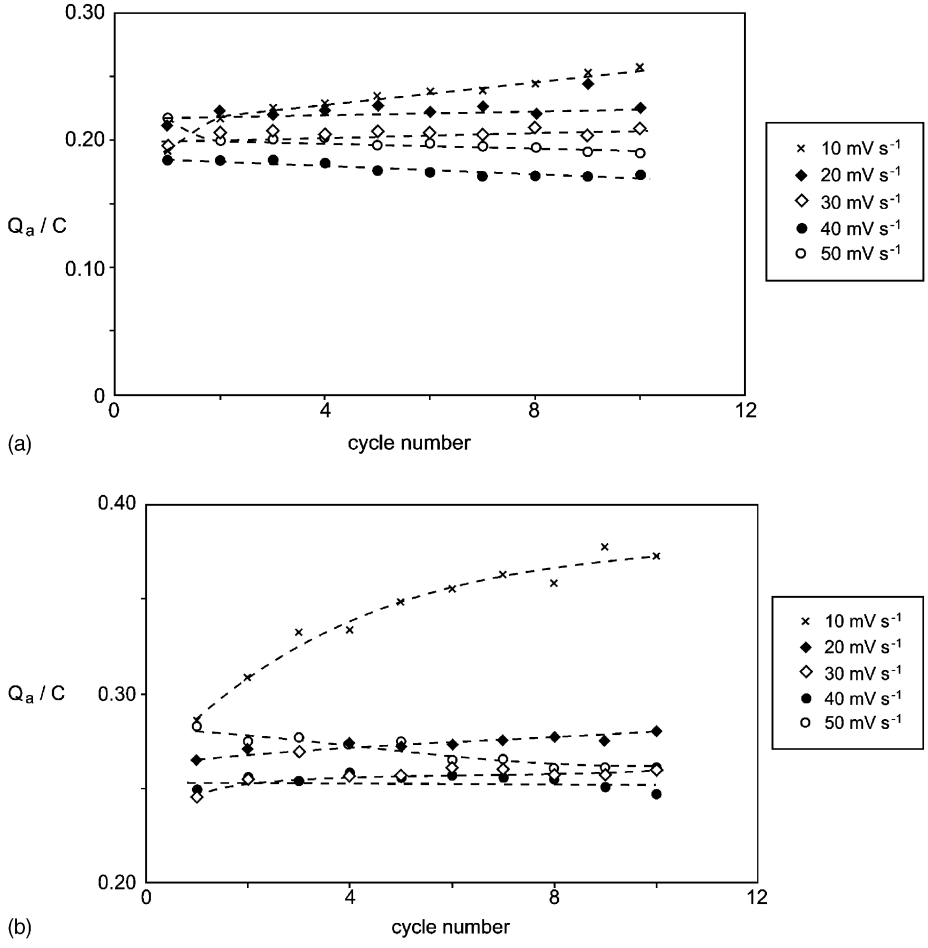

Fig. 4. (a) The dependence of anodic charges, Q_a, obtained at various sweep rates (10–50 mV/s), on a number of scans for Pb electrode in 0.5 M H_3PO_4. (b) The dependence of anodic charges, Q_a, obtained at various sweep rates (10–50 mV/s), on a number of scans for Pb electrode in 1.0 M H_3PO_4.

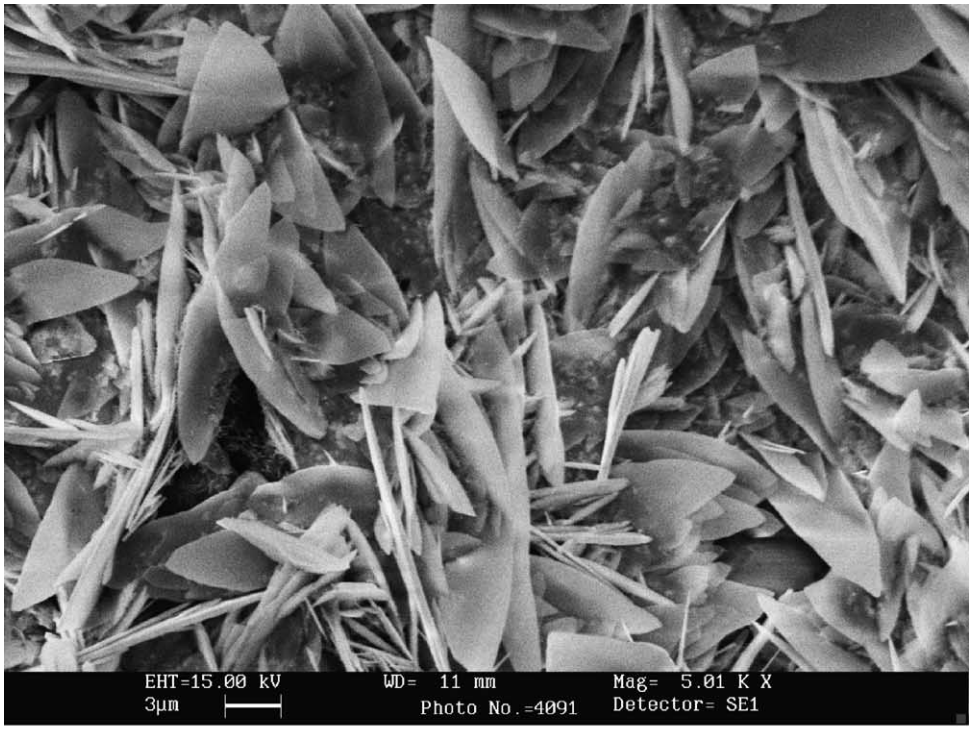

(a)

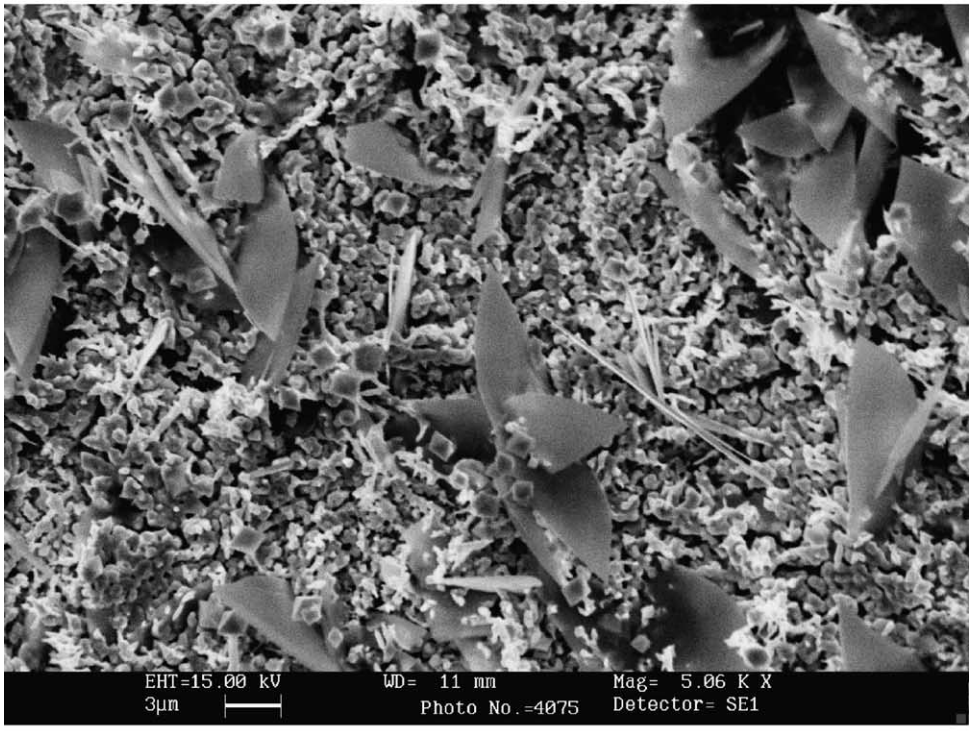

(b)

Fig. 5. (a) The SEM of Pb electrode in 0.5 M H_3PO_4 after oxidation at 0 V. (b) The scanning electron picture of Pb electrode in 0.5 M H_3PO_4 after reduction at −1.7 V followed by oxidation at 0 V.

polarization at the reduction potential. The SEM images (Fig. 5a and b) support the conclusion that the reduction process of lead(II), formed during the electrode polarization is not completed.

Cyclic voltammograms of a pure Pb-wire electrode in aqueous phosphoric acid solutions (0.5–5.0 M) in the potential region between hydrogen and oxygen evolution at a constant sweep rate (50 mV/s) are shown in Fig. 6a and b.

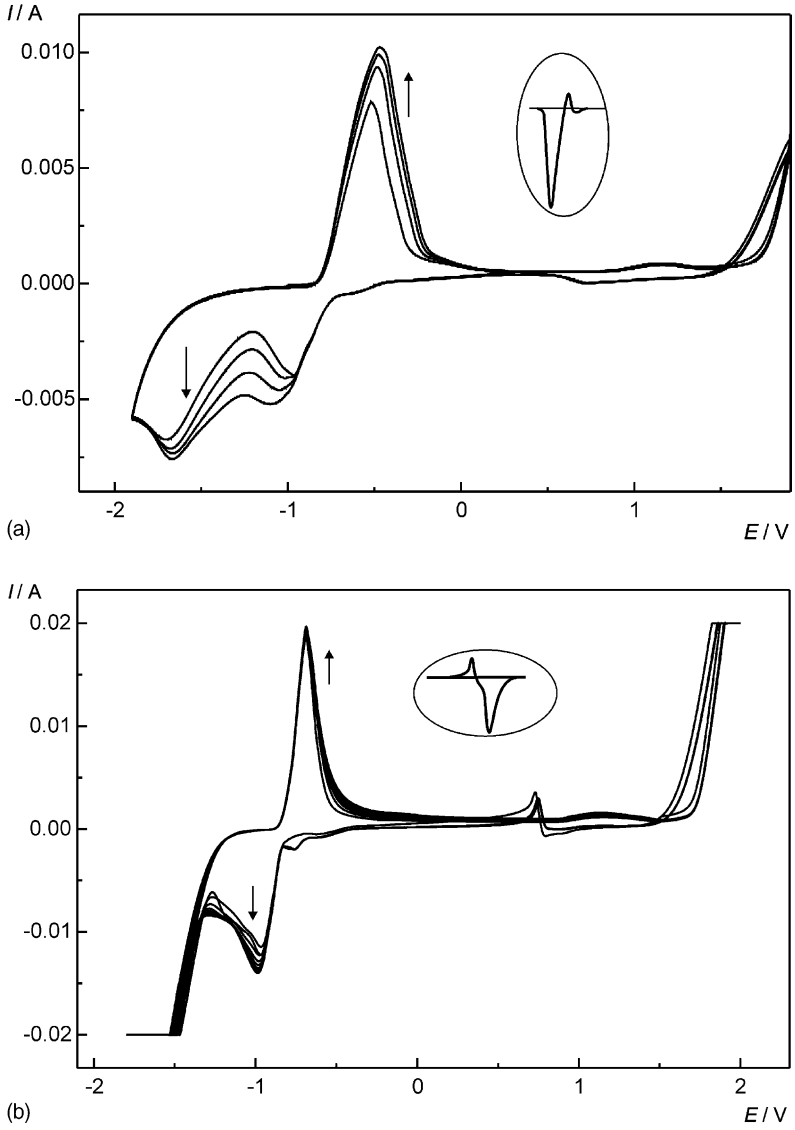

Fig. 6. (a) Voltammograms of Pb electrode in 0.5 M H_3PO_4 at 50 mV/s. In the circle, the ''anodic excursion'' peak location in 0.5 M H_2SO_4 is shown. The arrows indicate the order of cycle number. (b) Voltammograms of Pb electrode in 5 M H_3PO_4 at 50 mV/s. In the circle, the ''anodic excursion'' peak location in 5 M H_2SO_4 is shown. The arrows indicate the order of cycle numbers.

Also, in this figure are shown, in separated circles, ''anodic excursion'' peaks, which appear in sulfuric acid solution at a sweep rate of 50 mV/s.

A strong influence of the phosphoric acid concentration on the shape of cyclic voltammograms of lead is observed. Also, the currents responsible for surface reactions, i.e. lead oxidation–reduction currents are changed in comparison to the experiments performed in sulfuric acid solutions; especially the currents of oxidation–reduction lead(II) ⇔ lead(IV) processes are decreased. Only at higher phosphoric acid concentrations (5.0 M), is the ''anodic excursion'' peak present. Similarly to the behavior in 5 M H_2SO_4, it is located after the PbO_2 reduction process. In less concentrated sulfuric acid solutions (0.05 M) this effect also disappears [15].

Figs 7a and b show the voltammograms obtained for Pb electrode in 5 M sulfuric acid with various additions of phosphoric acid (2 and 10%).

The shape of the ''anodic excursion'' currents for both concentrations of phosphoric acid (2 and 10%) in 5.0 M sulfuric acid are similar to the shape obtained in pure sulfuric acid (Fig. 1), although this effect at higher phosphoric acid concentration is decreased. The effect observed for higher phosphoric acid (10%) is similar to the one seen in pure 5 M phosphoric acid (Fig. 6a and b). It seems that these effects are not only due to high hydrogen concentration, but also are related to the composition of the surface compounds (mixture of lead(II) sulfates and phosphates) and the presence of surface lead oxides (α- and β-PbO_2).

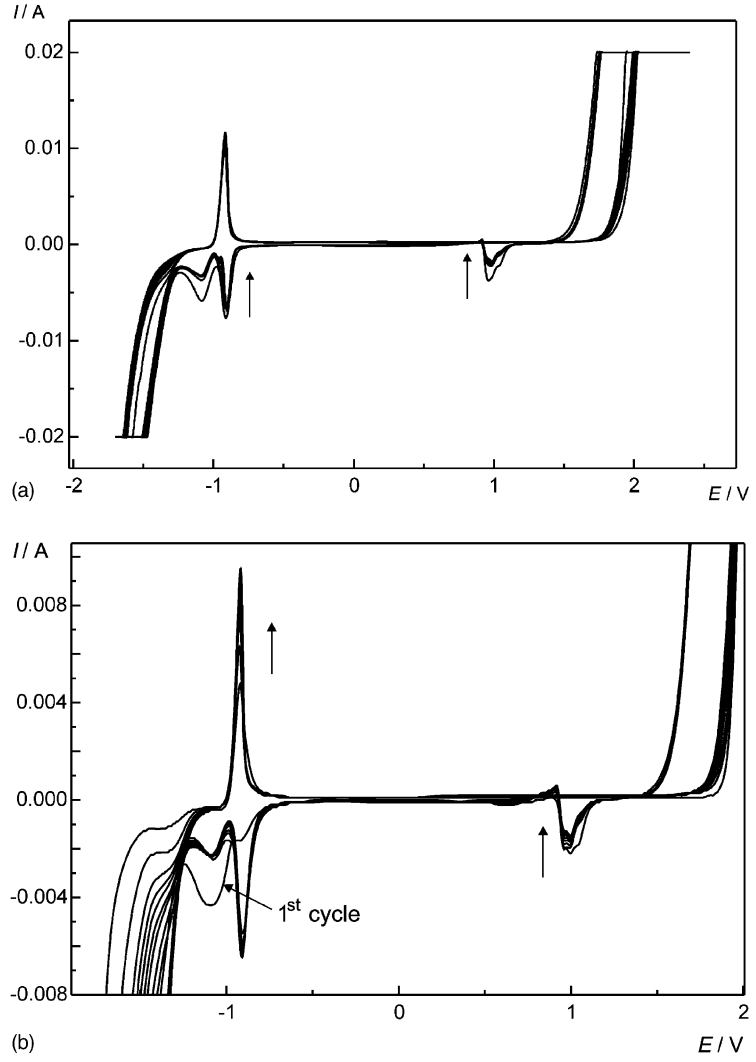

Fig. 7. (a) Voltammograms of Pb electrode in 5 M H_2SO_4 at 50 mV/s with the addition of phosphoric acid (2%). The arrows indicate the order of cycle numbers. (b) Voltammograms of Pb electrode in 5 M H_2SO_4 at 50 mV/s with the addition of phosphoric acid (10%). The arrows indicate the order of cycle numbers.

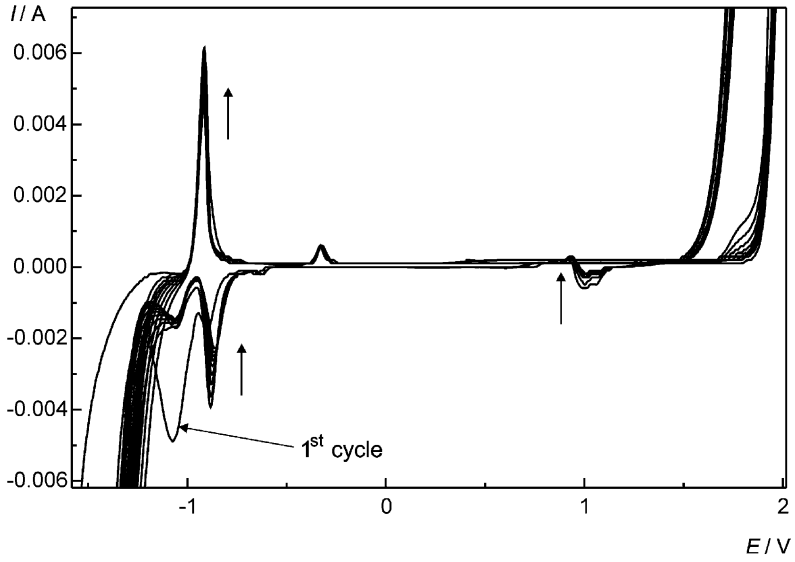

Fig. 8. Voltammograms of the Pb–Sb alloy (3% Sb) electrode in 5 M H_2SO_4 at 50 mV/s with the addition of phosphoric acid (10%). The arrows indicate the order of cycle number.

3.2. The electrochemical behavior of lead–antimony alloy in sulfuric and phosphoric acid solutions

The electrochemical behavior of lead antimony alloys is also in the area of interest of the electrochemical industry [19]. Fig. 8 shows the voltammograms of lead–antimony alloy (3%) obtained in 5 M sulfuric acid with the addition of phosphoric acid (10%).

These voltammograms were obtained without a preliminary Pb–Sb electrode polarization. Generally, they are similar to the curves presented in Fig. 7a and b; only a small oxidation peak at −0.3 V is observed due to antimony oxidation from the alloy. This peak of antimony oxidation from lead–antimony alloy is magnified and separated in Fig. 8. After a few scans, antimony is almost totally removed from the alloy surface. This results suggests that either Sb dissolves from the alloy surface during the first CV sweeps, or that it is connected with the formation of a $PbSO_4$ selective membrane.

It has to be noted that on the CV curves presented in Figs. 7 and 8, the currents of PbO_2 reduction are poorly visible.

Fig. 9a shows the voltammogram of lead–antimony (3% Sb) alloy obtained in 5 M sulfuric acid with the addition of phosphoric acid (10%) and Fig. 9b depicts the voltammogram of lead in 5 M phosphoric acid. In both cases the electrodes were initially polarized at 2 V before the experiments.

In both experiments, only during the first scan (starting from 2 V) are high reduction currents of PbO_2 to Pb(II) observed. In the next cycles, these currents significantly decrease. In both cases, an "anodic excursion" peak is still present on voltammograms. This effect is probably due to

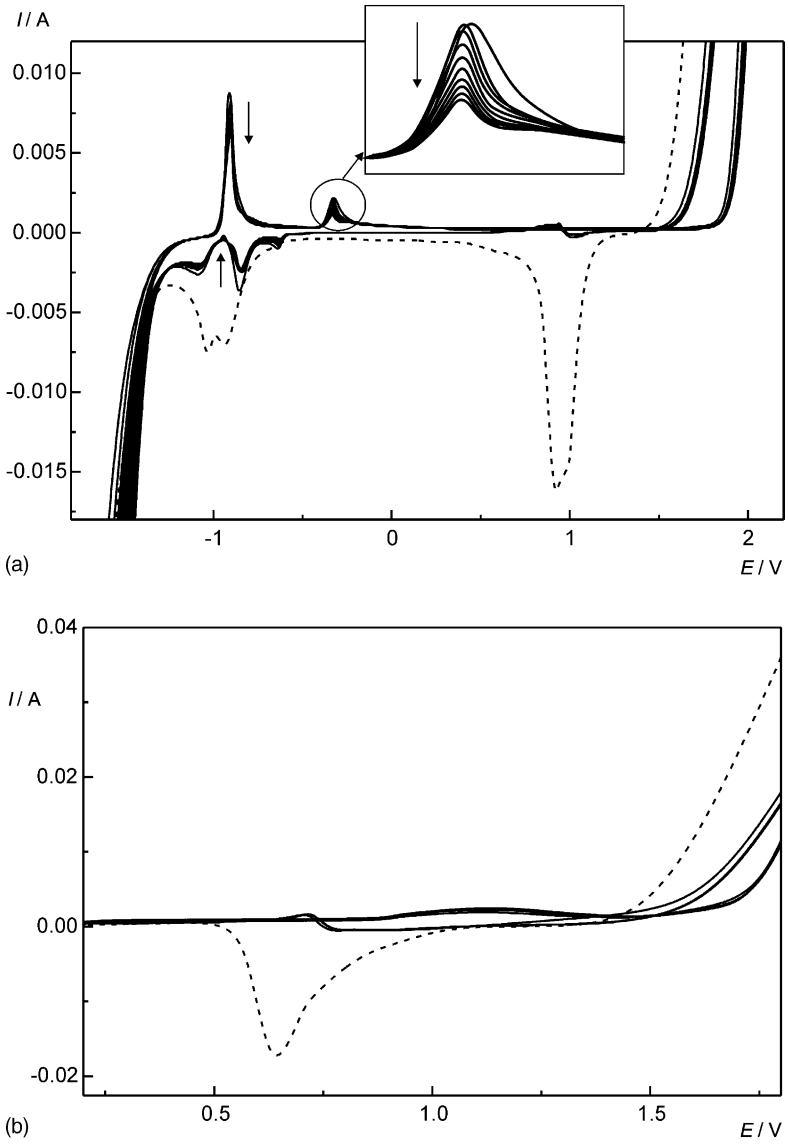

Fig. 9. (a) Voltammograms of the Pb–Sb alloy (3% Sb) electrode in 5 M H_2SO_4 at 50 mV/s with the addition of phosphoric acid (10%). Before the experiment the electrode was kept for 10 min at 2.0 V. The arrows indicate the order of cycle numbers. (b) Voltammograms of Pb electrode in 5 M H_3PO_4 at 50 mV/s with the addition of phosphoric acid (10%). Before the experiment the electrode was kept for 10 min at 2.0 V.

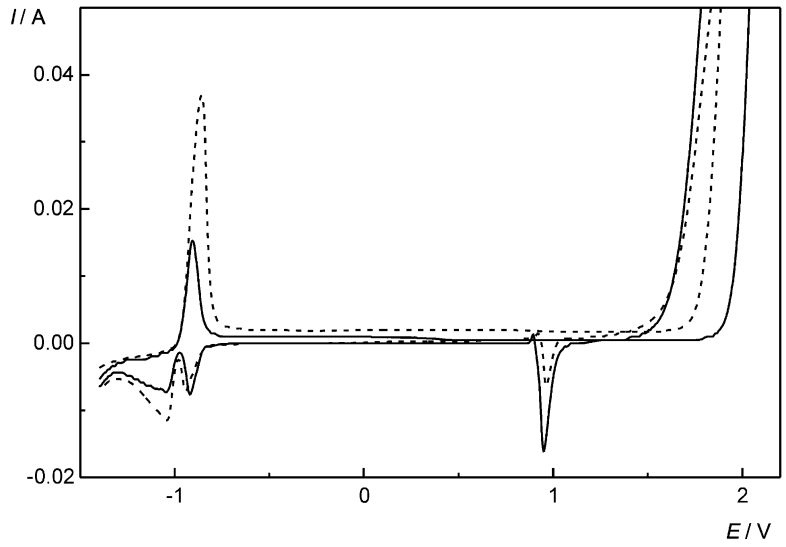

Fig. 10. Voltammograms of the Pb–Ca–Al–Sn alloy electrode (—) and Pb (- - -) electrode in 3 M H_2SO_4 at 50 mV/s.

lead phosphate formation which blocks the lead surface to PbO_2 oxidation. We can suggest that the presence of the ''anodic excursion'' peak is due to surface changes during phosphate formation from PbO_2, similarly to the mechanism which occurs during lead electrode polarization in sulfuric acid.

3.3. The electrochemical behavior of lead–calcium–aluminum–tin alloy in sulfuric and phosphoric acid solutions

For lead–calcium–aluminum–tin alloys the observed effects were similar to the ones seen for pure lead electrodes (Fig. 10). Only the ratios between the current values are different when the processes are generated at more positive or at more negative potentials in the case of pure lead and lead–calcium–aluminum–tin alloy electrodes.

4. Summary

The results of the study of the electrochemical behavior of lead and its alloys with antimony and other metals lead to the following conclusions regarding the nature of these redox processes:

1. The surface processes of lead during cyclic polarization processes in sulfuric and phosphoric acids are not fully reversible. Such irreversibility of the reactions leads to changes of the roughness factor and/or to incomplete reduction of the oxidation compounds formed on the electrode surface.
2. Only at higher phosphoric acid concentrations (5.0 M), is the ''anodic excursion'' peak present on voltammograms. Similarly to the behavior in 5 M H_2SO_4, it is located after the PbO_2 reduction process. In less concentrated phosphoric acid solutions this effect does not exist.
3. During cyclic polarization of lead–antimony alloys either Sb dissolves from the alloy surface during the first CV sweeps, or a selective $PbSO_4$ membrane is formed.
4. In sulfuric acid with phosphoric acid additions, the phosphate formation blocks the lead surface to PbO_2 oxidation. The presence of an ''anodic excursion'' peak is due to surface changes during phosphate formation from PbO_2, similarly to the mechanism which occurs during lead electrode polarization in sulfuric acid.
5. For lead–calcium–aluminum–tin alloys only the ratios between the densities of currents generated during oxidation and reduction are different in comparison to pure lead.

Acknowledgements

This work was financially supported by Warsaw University (120-521/68-BW-1522/16/2001). Financial support for A. Czerwiñski from Grant No. 8T 10A 03220 of Polish State Committee for Scientific Research (KBN) is also gratefully acknowledged.

References

[1] H.S. Panesar, in: D.H. Collins (Ed.), Power Sources, Vol. 3, Oriel Press, Newcastle-upon-Tyne, 1971.
[2] J.G. Sunderland, J. Electroanal. Chem. 71 (1976) 341.
[3] S. Fletcher, D.B. Matthews, J. Electroanal. Chem. 126 (1981) 131.
[4] R.L. Deutscher, S. Fletcher, J.A. Hamilton, Electrochim. Acta 31 (1986) 585.
[5] T. Laitinen, B. Monahov, K. Salmi, G. Sunholm, Electrochim. Acta 36 (1991) 953.

[6] T. Laitinen, K. Salmi, G. Sunholm, B. Monahov, D. Pavlov, Electrochim. Acta 36 (1991) 605.
[7] P. Matesco, N. Bui, P. Simon, J. Electrochem. Soc. 144 (1997) 443.
[8] M. Metikos-Hukovic, R. Babic, S. Omanovic, J. Electroanal. Chem. 374 (1994) 199.
[9] Y. Yamamoto, K. Fumino, T. Ueda, M. Namu, Electrochim. Acta 37 (1992) 199.
[10] Y. Yamamoto, M. Matsuoka, M. Kimoto, M. Uemura, Ch. Iwakura, Electrochim. Acta 41 (1996) 439.
[11] E.N. Corado, J.R. Vilche, Electrochim. Acta 42 (1997) 549.
[12] V. Danel, V. Plichon, Electrochim. Acta 28 (1983) 781.
[13] T. Laitinen, J. Pippo, T. Saario, M. Bojnov, B. Mohanov, in: Proceedings of the International Conference on Lead-Acid Batteries, Labat 96, Varna, 1996 (Abstract No. 22).
[14] Y. Gou, Z. Wei, S. Hua, Electrochim. Acta 42 (1997) 979.
[15] A. Czerwinski, M. Zelazowska, M. Grden, K. Kuc, J.D. Milewski, A. Nowacki, G. Wójcik, M. Kopczyk, J. Power Sources 85 (2000) 49.
[16] R. Babic, M. Metikos-Hukovic, N. Lajgy, S. Brinic, J. Power Sources 52 (1994) 17.
[17] T. Hirasawa, K. Sasaki, M. Taguchi, H. Kaneko, J. Power Sources 85 (2000) 44.
[18] L. Hou-Tiana, Y. Jionga, L. Hai-Hea, Z. Ji-Huaaa, Z. Wei-Fanga, J. Power Sources 93 (2001) 230.
[19] I. Peterson, E. Ahlberg, J. Power Sources 91 (2000) 143.
[20] S. Zhong, J. Wang, H.K. Liu, S.X. Dou, M. Skyllas-Kazacos, J. Power Sources 66 (1997) 107.
[21] S. Zhong, J. Wang, H.K. Liu, S.X. Dou, M. Skyllas-Kazacos, J. Power Sources 66 (1997) 159.
[22] M. Metikos-Hukovic, M. Babic, S. Brinic, J. Power Sources 64 (1997) 13.
[23] P. Mattesco, B. Nam, P. Simon, L. Albert, J. Power Sources 64 (1997) 21.
[24] S.S. Zhong, H.K. Liu, S.X. Dou, M. Skyllas-Kazacos, J. Power Sources 59 (1996) 123.
[25] S. Brinic, M. Metikos-Hukovic, R. Babic, J. Power Sources 55 (1995) 19.
[26] P. Simon, N. Bui, N. Pebere, F. Dabosi, L. Albert, J. Power Sources 55 (1995) 63.
[27] N.E. Bagshaw, J. Power Sources 53 (1995) 25.
[28] H. Giess, J. Power Sources 53 (1995) 31.
[29] L.A. Yolshina, V.Y. Kudyakov, V.G. Zyryanov, J. Power Sources 78 (1999) 84.
[30] S.C. Lakshmi, J.E. Manders, D.M. Rice, J. Power Sources 73 (1998) 23.
[31] W. Guo-Lina, W. Jia-Ronga, J. Power Sources 52 (1994) 25.
[32] J. Garche, H. Doring, K. Wiesener, J. Power Sources 33 (1991) 213, , and references therein.
[33] W. Visscher, J. Power Sources 1 (1976/1977) 257.
[34] E. Voss, J. Power Sources 24 (1988) 171.
[35] M. Chatelut, S. Chah-Bouzziri, O. Vittori, A. Benayada, J. Solid State Electrochem. 4 (2000) 435.
[36] E. Meissner, J. Power Sources 67 (1997) 135.